Breaking Down the Energy Consumption of Industrial and Collaborative Robots: A Comparative Study

Heredia, Juan; Schlette, Christian; Kjærgaard, Mikkel Baun

Published in:
IEEE International Conference on Emerging Technologies and Factory Automation

Publication date:
2023

Document version:
Submitted manuscript

Citation for pulished version (APA):
Heredia, J., Schlette, C., & Kjærgaard, M. B. (Accepted/In press). Breaking Down the Energy Consumption of Industrial and Collaborative Robots: A Comparative Study. In *IEEE International Conference on Emerging Technologies and Factory Automation* IEEE.

Breaking Down the Energy Consumption of Industrial and Collaborative Robots: A Comparative Study

Juan Heredia[1], Christian Schlette[1] and Mikkel Baun Kjærgaard [1]

***Abstract*—Industrial robots have been widely used in diverse activities and industries for more than six decades. However, these robots were initially designed to operate autonomously without human interaction. The emergence of a new generation of manipulators, namely lightweight robots such as collaborative robots, has revolutionized the industry by enabling robots to work alongside humans. In this paper, we qualitatively compare the energy consumption of these two types of robots. First, we propose experimental setups to investigate how specific variables, such as standstill position, motion commands, velocity and acceleration limits, time scaling, and joint temperatures, influence the energy consumption of a cobot, namely, UR3e. Then, the cobot results are compared to IR experimental results which are mainly based on existing literature. The comparison reveals that the energy signature graph, which depicts the energy consumption versus execution time, differs between these two robots. Furthermore, industrial robots consume a considerably larger amount of mechanical energy compared to their electronic components' energy, while cobots consume a higher proportion of energy in their electronic components. Energy optimization strategies for cobots should focus on efficient electronic design, such as the distribution of computation tasks among system assets, rather than reducing energy consumption through motion planning.**

***Index Terms*—Energy aware automation; Collaborative Robots in Manufacturing; Sustainability and Green Automation.**

I. INTRODUCTION

The International Organization for Standardization defines an industrial robot as an "automatically controlled, reprogrammable multipurpose manipulator programmable in three or more axes" [1]. Industrial robots (IRs) have revolutionized the industry due to several production advantages, including improved productivity (increased production and decreased production time), energy and resource efficiency (optimized performance resulting in reduced energy consumption and material waste), improved production quality, and increased flexibility and adaptation to changes in production structure [2]. The car manufacturing industry was the first to introduce robots to their production lines. At the GM Ternstedt plant in Trenton, NJ, the first industrial robot was introduced to a production line that manufactured automotive hardware such as door and window handles, gearshift knobs, and light fixtures [3]. Nowadays, industrial robots are one of the principal components of any modern industry. According to the International Federation of Robotics (IFR), sales of industrial robots have grown by 31% in 2022, with 517,385 units sold. The principal industrial sectors where robots have been installed include electrical/electronics, automotive, metal and machinery, plastic and chemical products, food, and others [2].

[1]Authors are with the Mærsk Mc-Kinney Møller Institute, University of Southern Denmark, Odense, Denmark jehm@mmmi.sdu.dk, chsch@mmmi.sdu.dk, mbkj@mmmi.sdu.dk

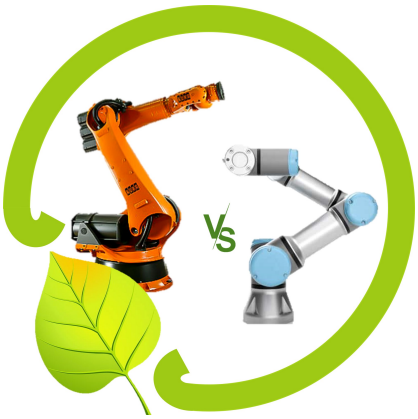

Fig. 1. Energy Consumption of Cobots and Industrial Robots.

A new generation of lightweight industrial manipulators (LIRs) called "Collaborative Robots" appeared in the last few years. This generation is designed to move in the same working environment with operators (without fences) due to safety protocols (ISO 10218) [4]. Also, these robots are not only designed to move objects but also to perform dexterous applications like inserting a screw or assembling electronic boards. Traditional industrial robots are still more used than collaborative robots (478 000 industrial robots and 39 000 collaborative robots were installed in 2021). However, the number of new collaborative robots is increasing increased by 50 % in 2021. [2]

In the literature, authors have focused their attention on the performance analysis of industrial robot (IR) energy consumption (EC). Although cobots and IRs share a similar structure, their performance can differ due to several factors, such as: 1) Cobots are built using flexible and lightweight materials that can absorb energy in case of a collision [5]. 2) Cobots obey safety protocols that reduce the risk of collisions with operators, such as speed and acceleration limits [4]. In contrast, IRs are usually inside fences and can work using the maximum possible velocity and acceleration. 3) Constituent parts, such as the type of motors and brakes, differ between cobots and IRs. Cobots are designed using small and lightweight components [6]. Thus, cobots are lightweight structures that move slowly with miniaturized and lightweight components, causing a change in the manipulator's dynamic behavior. The energy consumption (EC) of these two kinds of robots is expected to differ. In this paper, we present a framework that analyzes cobots' EC using the same criteria as previous studies on IRs and qualitatively compares the EC of both robots. By examining these differences, we can gain insights into the relative performance of cobots and IRs and better understand how each technology can be best applied in

different industrial contexts.

This paper is organized as follows. In Section II, a literature review of the most important work on energy assessment of industrial robots is presented. Section III addresses the overall approach, and describes performance metrics and experimental procedures. In Section IV, the differences and similarities between IRs and cobots are discussed. Finally, Sec. V concludes the paper.

II. State of the Art

A. IRs and Cobots

In recent years, there has been a growing interest in comparing traditional industrial robots (IRs) and industrial collaborative robots (cobots) due to their increasing prevalence in the manufacturing industry. These studies have utilized various parameters for comparisons, such as mechanical and software design, safety features, user interface, and applications [5], [6]. Overall, these comparative studies are valuable for identifying the strengths and weaknesses of both types of robots and can help guide the development of more efficient, safe, and user-friendly robotic systems.

IRs are heavy and typically require installation in a fixed mounting structure, often within a cage. This leads to longer installation times and higher costs. For instance, the Kuka series and ABB series for industrial robots have specific installation requirements such as concrete or mounting forces specifications [7]–[10]. In contrast, cobots are lightweight and easy to install, without requiring any modification of the workspace [11]–[13]. This makes cobots a more flexible and cost-effective solution for a variety of industries [14]. However, it's important to note that cobots generally have a smaller payload capacity than IRs.

Although the mechanical design of IR and cobots is similar, their joint mechanisms differ. Industrial robots (IRs) have traditionally relied on pneumatic, hydraulic, or electrical actuators to function [15]. In contrast, cobots have embraced modern electrical actuators like induction brushless DC motors [16]. Furthermore, transmission systems are crucial for transferring mechanical power from the motor to the load. While IRs have traditionally utilized direct drives, band drives, belt drives, or gear drives [15], almost all cobots prefer worm fear drives such as harmonic drives, due to their lightweight and compact design [17], [18].

IRs generally are designed with six degrees of freedom (DoF), while there are cobots with six or seven DoF [6]. Cobots are built for applications requiring dexterous manipulation. Their increased DoF allows for more flexibility and adaptability to different tasks, making them a popular choice in industries with varying needs [14].

The sensors that an IR uses are related to its performance, namely, encoders, motor torque, and current sensors. Cobots by contrast need additional sensors to detect collisions with operators and perform interaction tasks where cobots and humans safely interact [19].

IRs require a specialist to program them due to the nature of their antiquated, imperative programming languages [20], and typically these programs are written offline for safety purposes [21]. Cobots, by contrast, are characterized by their user interface which significantly differentiates them from IRs [22]. The goal of cobot manufacturers is to design interfaces that allow non-specialists to program robots easily. In terms of user experience, [22] lists four distinct approaches: cobot teaching pendants, icon-based programming, CAD-based programming, and task-based programming. Alongside these methods, researchers have explored newer technologies like teaching by demonstration, Kinaesthetic teaching, and teleoperation when it comes to cobot programming [23], [24].

IRs use safeguards by separating robots from human reaches, while cobots use safety mechanisms to ensure safe collaborations in a shared workspace [25]. In the case of cobots, the robot standard ISO 10218-1/2:2011 presents four collaborative modes, namely, safety-rated monitored stop, hand guiding, speed and separation monitoring, and power and force limiting [4].

IRs and cobots have an important role in modern industry, however, these robots have different tasks. IRs are used for assembling, surface coating, welding, laser cutting, machine loading, or palletizing [6]. In the contrast, cobots are used on applications like co-manipulation in assembling, picking and placing, inspection, and screwing [22].

B. Energy Assessment of IRs

Many authors have analyzed the EC of IR using experimental campaigns and simulations to determine the relationship between robot parameters and its EC. The studies have used robot variables such as velocity limit, acceleration limit, payload weight, trajectory, robot status, and joint temperature. All the literature has focused on experiments for IRs.

TABLE I
Comparative analysis between Cobots and IRs.

Criteria	Industrial Robot	Industrial Collaborative Robot
Mechanical and Software Desing	Pneumatic, hydraulic and electrical actuators	Typically Induction brushless DC motors
	Fixed installation Usually 6-axis with last three intersecting in wrist Setting up takes days or over weeks	Flexibly Relocation Usually 6 or 7-axis Quick set up
Programming	Online and off-line programming by a robot specialist	Online instructed by a process expert and supported by offline methods
Safety	Rarely interaction with the human, only during programming	Frequent interaction with the human, even force/precision assistance
	Human and robot separated through perimeter safeguarding Hazards prevented by not allowing access	Workspace sharing with human Requested risk assessment
Applications	No ability to provide support to the human	Provide power support to the human
	Assembly, surface coating, welding, laser cutting, machine loading, palletizing	Manipulation, process tasks, pick and place, and inspection

We intuitively infer that the EC depends on the robot's position (static or dynamic), and authors have proved this relationship in [26], [27]. Garcia et al. [26] presented four common standstill positions and selected the optimal standstill robot position from this group. Moreover in [27], the authors compared the robot EC performing the same trajectory on different working planes. The authors concluded that EC does not only depend on the trajectory but also on the robot's working plane.

In a dynamic state, the EC of an IR depends on many variables. We observe four variables: trajectory, brakes' releasing, joint temperatures, payload, and energy regeneration from previous work. Variables such as velocity and acceleration limits have been included in the trajectory since these parameters directly modify the trajectory.

Different research groups [26]–[33] have deeply analyzed the relationship between acceleration and velocity limits to the EC. In [28], the experiments demonstrated that too big or small velocity and acceleration limits increase the EC. Even in [32], [33] the authors mentioned that the EC is optimized by minimizing the squared sum of the acceleration. Besides in [30], [31], Gandaleta et al. presented an analysis of the acceleration and velocity limits. Using the experimental data, the authors plotted a color map to characterize the EC of a determined trajectory in a given robot. Additionally, the authors found a relationship, called energy signature, between EC and motion time.

Among the contributions that analyze how the robot trajectory affects EC, Vegnano et al. [34] proposed the energy signature concept. The energy signature represents the EC as a function of the motion time, which mathematically is a fourth-order equation. Moreover, the function is generated by scaling the time based on an initial trajectory or modifying the velocity and acceleration limits. Afterward, many authors [26], [30]–[32], [35] have performed experiments in other robot brands, obtaining similar curve characterization.

The payload influence on the EC is evident. When the payload weight increases, the robot consumes more energy. In [26]–[29], [35], [36], analyzed and quantified the EC increment. These studies suggest that the analysis should be performed in static and dynamic positions.

The temperature of the motors has been examined in [26], [31]. The motors of IR have intensive EC and operate in high temperatures. The experiments showed a correspondence between the EC and the temperature. The EC is inversely proportional to the temperature. However, it is necessary to test the hypothesis using a cobot. Since a cobot possesses lighter, less powerful motors, the relationship might change or even not exist.

The last parameter analyzed in the literature [26], [30], [31], [37] is the release of joint brakes, which are mechanisms used to maintain the robot's position. In IR, the brake release can be programmed. However, some of the cobot manufacturers (for example, Universal Robots) do not provide access to control the brakes.

In this paper, we propose a new methodology to assess the EC of cobots. The methodology compiles the evaluation parameters found in the literature related to cobots. The selected evaluation parameters are joint configurations, joint temperatures, payload, movement command, acceleration limit, velocity limit, and trajectory planning. Besides we present a case study to demonstrate the methodology application.

III. ENERGY ASSESSMENT

This section presents experimental setups to evaluate the EC of a cobot. The results of the tests are qualitatively compared to the results of an IR. The robot UR3e is selected to contrast with IRs because UR3e is one of the smallest cobots on the market.

To perform the experiments, we need the following sensors and instruments, as it is shown in Fig.2.

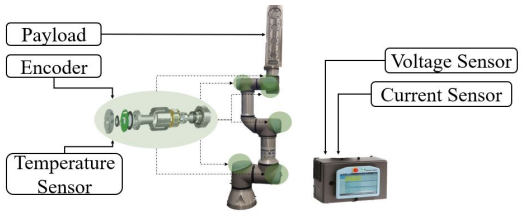

Fig. 2. Materials for energy assessment experiments.

A. Standstill

This test is designed to study the robot's EC performance while it waits at a standstill position to start a new movement, i.e, the robot's brakes are open or released, and the robot joint is free to move. Unlike IRs, LIR's controller does not have commands to close and open brakes by software due to safety protocols. Activation and deactivation of brakes are done using its teaching pendant or web application. In [26], four joint configurations which are most common to be used in an industrial environment were presented. This experiment measures the EC in these different joint configurations (see Fig. 3).

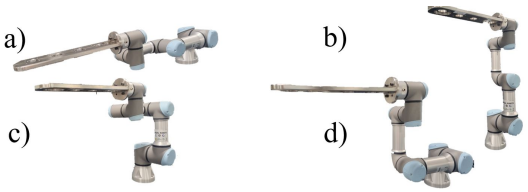

Fig. 3. Recommended standstill positions for anthropomorphic robots [26].

Table II presents a descriptive statistics table for each configuration's power consumption. The results indicate that Configuration a (52.23 W) consumes the most energy, while Configuration b (45.42 W) consumes the least amount of energy.

TABLE II
POWER CONSUMPTION ON STANDSTILL POSITION.

	Mean[W]	STD[W]	Min[W]	Max[W]
Config. a	52.2308	2.3063	46.9096	60.2568
Config. b	45.4214	1.8764	41.0140	50.2089
Config. c	52.1604	2.2884	47.0369	57.9741
Config. d	47.2521	1.9237	43.0455	52.4802

One-way ANOVA and the Tukey Honestly Significant Difference tests were performed to determine any statistical difference between the four configurations. The one-way ANOVA test revealed that there was a statistically significant difference in mean power consumption between at least two groups ($F(3,396) = [270.05]$, $p < 0.05$). Tukey's HSD Test for multiple comparisons indicates that Configuration a (52.23 W) consumes the most energy, while Configuration b (45.42 W) consumes the least amount of energy.

B. Command Motion

Test Setup: The robot moves back and forth between point P_1 to point P_2 lifting its maximum payload capacity using the manufacturer's generic trajectory commands, e.g., joint linear movement (or Point to Point (PtP)) and Cartesian linear movement. The points P_1 and P_2 are defined by the ISO norm 9283:1998 (see Fig. 5). The points P_1 and P_2 are placed at the points (150, -100, 100) mm and (450, 100, 300) mm, respectively. The velocity linear limits are set in the range from 0.15 to 1.5 $[m/s]$ with an interval of 0.15 $[m/s]$ for linear movements. In the case of PtP movements, the range of values is between 0.3 to 3 $[rad/s]$ with an interval of 0.3 $[rad/s]$. The payload is 3 kg.

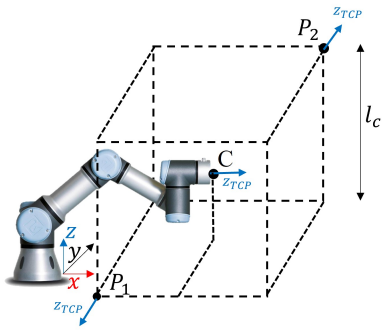

Fig. 5. Cube for performance tests based on ISO 9283:1998 Manipulating industrial robots — Performance criteria and related test methods [38].

Results: Fig. 4 shows the EC for PtP and linear movements from P_1 to P_2 forward and backward. The top subfigures show an EC map, which illustrates the EC tendencies of each movement. We plotted all the experimental points (EC versus execution time) and observed a linear trend. Then, a linear regression model is generated and evaluated using R^2 and the ANOVA test, which yielded statistical results of $R^2 > 0.999$ and $p_{value} < 0.05$. The results showed that the robot's EC is directly proportional to the execution time.

Type of motion: The equation ΔEC is the difference between the linear command's EC and the PtP command's EC, such that

$$\begin{aligned} \Delta \text{ EC} &= EC_{LinearMov} - EC_{PtP} \\ &= \text{-2.29} \quad \text{t} + 55.45 \quad , \end{aligned} \tag{1}$$

where EC_{PtP} and $EC_{LinearMov}$ are the EC model equations for PtP and linear commands. The equilibrium point, where Linear and PtP commands consume the same energy, is found at $\Delta EC = 0$, such that, the time is 24.21 s. Based on the numerical solution, we determined that the PtP command uses less energy in fast movements ($t < 24.21\,s$) while the linear command uses less energy in slow movements ($t > 24.21\,s$).

Payload: Robot's EC evidently increases when the robot lifts a maximum payload. To understand the effect of the payload on the robot's EC, the previous experiment without a payload and find the energy increase percentage is repeated, i.e., the robot UR3e moves fordward and backward between point P_1 and P_2 using its maximum velocity and acceleration. The experiment was repeated 30 times to avoid outliers in the dataset.

Fig. 7 presents the average EC for cartesian linear and PtP motion while the robot lifts a payload and without a payload. The percentage difference between the EC with and without payload is 9.35 and 10.66 for cartesian linear and PtP commands, respectively.

Controller Energy and Teaching Pendant Consumption: The controller energy is measured using the power analyzer HMC8015. The manipulator is disconnected from the controller, and the power analyzer only measures the electrical power consumed by the controller and the robot teaching pendant. The controller and teaching pendant together consume 58.39 W.

C. Time Scaling

Test Setup: The trajectory is defined by a set of sinusoidal equations for each joint, such that,

$$\theta_i(t) = \theta_{0i} + A_i\, sin(2\,\pi\, f_i\, k\, t + \phi_i)\,, \tag{2}$$

where θ_i and θ_{0i} are the angular position and initial position of the i-articulation. The variables A_i, f_i, and ϕ_i are the trajectory parameters, while k is the time scaling variable. The trajectory parameters are defined, such that, the initial position vector is $\theta_0 = [0, -\frac{\pi}{2}, 0, 0, -\frac{\pi}{2}, 0]$ rad, the sinusoidal amplitude vector is $A = [2, 1, 1, 1, 1, 1]$ rad, the oscillation frequency vector is $f = [0.16, 0.5.1, 1, 1, 1]$ Hz, and the scaling factor vector is $k = 1, 1.2, ..., 2.8$.

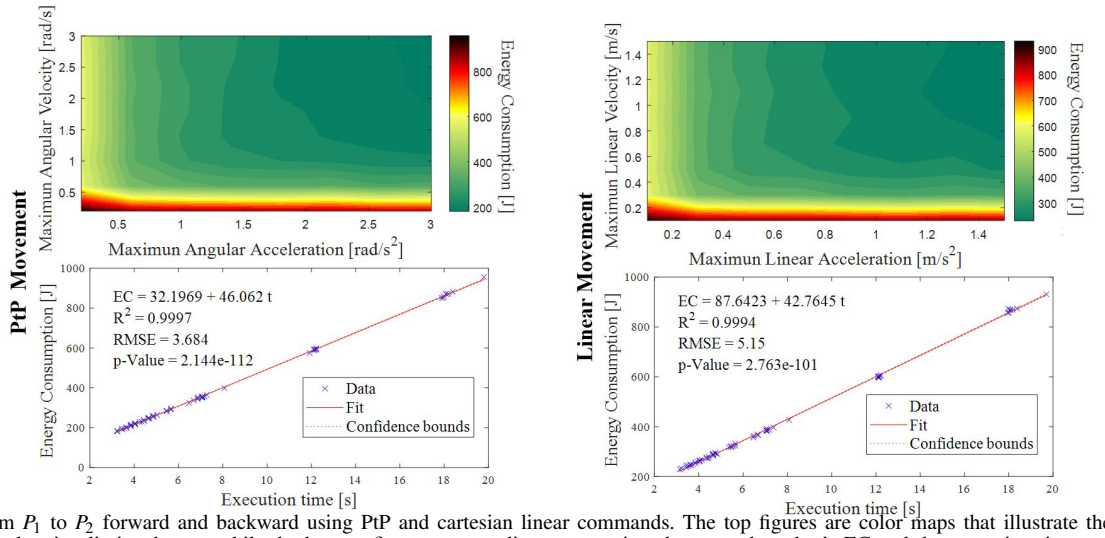

Fig. 4. EC from P_1 to P_2 forward and backward using PtP and cartesian linear commands. The top figures are color maps that illustrate the EC when the velocity and acceleration limits change, while the bottom figures present linear regressions between the robot's EC and the execution time.

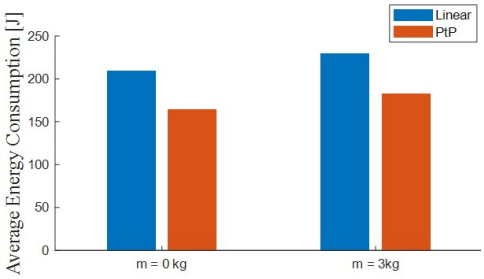

Fig. 7. Energy Consumption with and without payload for cartesian linear and PtP command.

The robot operates under two scenarios: constant experiment period or variable experiment period.

- Constant experiment period: the cobot should wait in a standstill position after finishing the experiment to maintain a constant experiment period. The EC during the standstill position is recorded as part of the experiment. For this test, the robot completes the path and waits to complete 60 s.
- Variable experiment period: the cobot executes continuous repetitions. After the robot finishes the path, it might wait at a standstill position to cool the joints. However, the EC in a standstill position is not recorded as part of the experiment. In the case of this experiment, the execution time is 20 s when the factor is ($k = 1$).

Results: Fig. 6 shows the EC of the robot over time for the two scenarios. In the waiting scenario (Fig. 6a), the EC between the different scale factors does not show any statistical difference. Hence, the EC does not depend on how fast the task is completed.

In the no-waiting scenario (Fig. 6b), the EC increases with an increase in the factor. We observe a linear dependency in the figure. Therefore, a linear regression model of EC is created, dependent on the execution time. The model was evaluated using R^2 and ANOVA tests, and the statistical results ($R^2 > 0.999$ and $p_{value} < 0.05$) indicate that the data fit a linear model perfectly. The results of Fig. 6c demonstrate that the EC depends on the scale factor.

D. Joint Temperature

Test Setup: This experiment's objective is to determine how the temperature influences EC when all the joints are moving. This test uses sinusoidal joint movements (the same trajectory as the previous experiment (time scaling) with a factor (k=1.4)) during 500 [s] in warm and cold conditions.

- Cold Conditions: Immediately, after the robot is turned on, the robot executes this trajectory.
- Warm Conditions: The robot should have been operative with the robot's run time on this day being $\approx$ 30 min. Then, the robot executes the same trajectory.

Results: Table III summarizes the EC and the joint temperatures during the experiment under cold and warm conditions. Fig.8 shows a snap capture of the first 30 [s] of the experiment. We observe that the robot consumes slightly less energy when the robot is warm.

TABLE III
EC OF THE ROBOT AT DIFFERENT MOTOR'S TEMPERATURE CONDITIONS

	EC[kJ]	Joint Temperatures [°C]					
		1st	2nd	3rd	4th	5th	6th
Cold	36.83	27.86	27.92	29.32	32.06	32.46	32.28
Warm	35.34	36.52	38.50	40.13	42.66	44.64	44.02

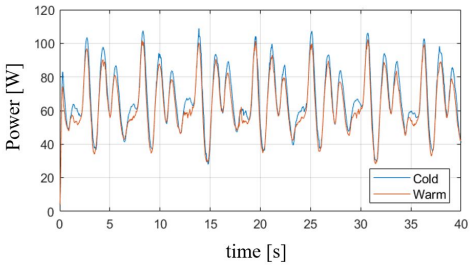

Fig. 8. Snap shot of the first 30 S of the experiment under cold and warm conditions. The robot's EC slightly reduces under warm conditions.

A paired-sample t-test was performed to compare robot power profiles with and without payload in cold and warm conditions. There was a significant difference in the robot power profile without payload between cold and warm conditions (t(27997) = 168.27, p = 0). Also, there was a significant difference in the robot power profile with payload between cold and warm conditions (t(27997) = 193.84, p = 0). The experiment results and statistics suggest that the joint temperatures modify the robot's EC. Our results indicate that EC decreases when the robot is under warm conditions.

IV. COMPARISON BETWEEN COBOT AND IR ENERGY CONSUMPTION

This section compares the EC behavior of various IRs from the literature to experimental results obtained with the UR3e. However, in order to gain a more comprehensive understanding of EC behavior, further extensive studies should be conducted using other cobot designs and manufacturers.

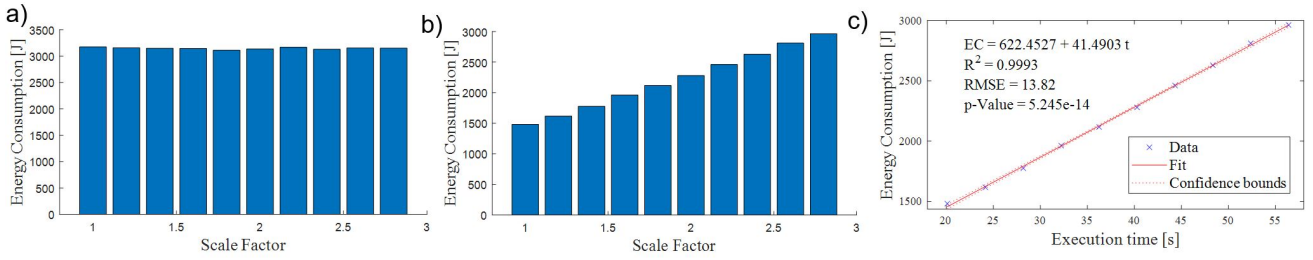

Fig. 6. The results of Test III, which involved the scaling factor, are presented. Fig. a shows the results of the waiting scenario, where the EC is almost constant, and the statistical analysis does not reveal any significant differences. On the other hand, Fig. b and Fig. c illustrate the EC in the no-waiting scenario, where the EC is linearly dependent on the execution time.

The results from the above section were compared to those obtained by other authors in previous papers. Table IV compares the energetic behavior of a cobot and an IR, applying the proposed criteria (payload, joint configurations, movement commands, velocity and acceleration limits, trajectory planning, and joint temperatures). The comparative analysis focuses on determining the influence of the above evaluation criteria on robot EC. IRs have higher payload capacity, velocity, and acceleration limits; therefore, IRs evidently consume more energy than cobots. Quantitative analysis of the EC on the different scenarios would reflect that IRs consume more energy. Normalized metrics are used to perform a qualitative analysis of the evaluation parameters' influence.

A. Standstill position

IRs and cobots are influenced by the joint configuration of their joints. In [26], the results demonstrate that the joint configuration strongly influences its EC. In the case of UR3e, the joint configuration also influences the EC. The test "Standstill position" demonstrated that 13.94 % of the energy can be reduced by placing the robot in an efficient standstill position.

IRs use joint brakes to hold the position for long standstill times. While IRs have their brakes released, the robot EC is the energy required by the controller and joint electronic components. In contrast to IRs, cobots can not activate their brakes programmatically. The EC in standstill is the energy required by the motors to hold their position, the controller, and the joint electronic components.

B. Motion Command

In this comparison, the article [31] presents an extensive analysis of the influence of the motion command and payload on IR consumption (KUKA KR210 R2700 + KUKA KRC4). The dataset of these experiments is available in [41], and is used to compare with UR3e performance. In Table V, the EC dataset of both robots and a set of metrics that compare the EC factors are presented.

Velocity and Acceleration Limits: In the case of UR3e, the EC peak is when the robot operates at its minimum velocity and acceleration limits. While in IR, the maximum EC is when the robot operates at its maximum velocity and acceleration limits. This difference is caused by the safety velocity and acceleration standard for cobots. These safety standards prohibit the robot to move using high speeds and accelerations harmful to operators in the environment.

Type of motion: The percentage difference between EC of cartesian linear EC_L and PtP EC_{PtP} commands is the metric that compares the EC of both robots using the following equation:

$$\phi_m = \frac{EC_L - EC_{PtP}}{(EC_L + EC_{PtP})/2}. \tag{3}$$

The results of this metric are presented in Table V. The UR3e robot consumes more energy when it uses cartesian linear commands, with a 24.13% increase in energy consumption without payload and a 22.87% increase with payload. When KUKA IR moves without payload, utilizing the cartesian linear command also results in a 4.37% increase in energy consumption compared to the PtP command. However, when the robot carries a payload, the KUKA IR utilizing the PtP command consumes 1.47% more energy than the cartesian linear command. The EC of both UR3e and KUKA IR robots varies depending on the type of commands given to them and whether they are carrying payloads or not.

Payload: The two robots have different payload capacities. IRs can move heavy payloads while cobot payload capacity is smaller. The ratio of the payload to the manipulator mass (ϕ_{PR}) is a metric used to compare the payload capacities of the two robots. The UR3e has a ratio of 0.27, while the KUKA KR200 has a ratio of 0.19, indicating that the UR3e has a relatively higher payload capacity than the KUKA KR200.

To compare the influence of the payload on the EC, the percentage difference on cartesian linear and PtP commands is used, such that :

$$\phi_p = \frac{EC_m - EC_0}{(EC_0 + EC_m)/2}, \tag{4}$$

where EC_m and EC_0 represent the EC with payload and without payload, respectively. The difference in EC between the two robots varies from 6% to 12%, indicating that the payload factor has a similar impact on both robots. In other words, increasing the payload has a comparable effect on the energy consumption of the UR3e and KUKA IR robots.

Electronics Components' Consumption: This parameter is analyzed by the percentage of energy used by the controller compared to the total energy used by the manipulator, such that

$$\phi_E = \frac{EC_E}{EC_E + EC_M}, \tag{5}$$

where EC_M and EC_E represent the EC of the manipulator, and electronic components (controller, teaching pendant), respectively. The results show that on average, 47.41% of the UR3e's energy is consumed by electronic components. In contrast, KUKA consumes only 5.94% of its energy on the controller and other electronic components. The percentage of energy consumption by electronics is one of the main differences between IRs and cobots. A significant portion of the total energy consumption of a cobot is attributed to the controller.

Fig. 9 presents a summary of the influence of factors such as payload-manipulator ratio, payload, electronics consumption, and type of command.

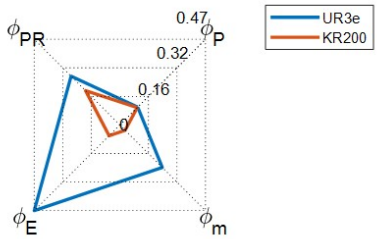

Fig. 9. EC metrics of UR3e and KR200.

C. Time Scaling

In a previous study [40], the authors introduced the Energy Signature graph, which illustrates the relationship between energy consumption and execution time (ET). This graph

TABLE V
THE RESULTS OF MOTION BETWEEN TWO POINTS USING MAXIMUM VELOCITY AND ACCELERATION LIMITS. [1]

		EC [KJ]		ϕ_p [%]	ϕ_E [%]	
	Payload	0 kg	3 kg		0 kg	3 kg
UR3e	**Linear**	0.209	0.229	9.35	45.6	43.34
	PtP	0.164	0.182	10.4	51.65	49.04
	ϕ_m [%]	24.13	22.87		$\overline{\phi_E}$ = 47.41	
	Payload	0 kg	133 kg		0 kg	133 kg
KUKA	**Linear**	18.7	20.0	6.72	6.10	5.70
	PtP	17.9	20.3	12.57	6.37	5.62
	ϕ_m [%]	4.37	-1.49		$\overline{\phi_E}$ = 5.94	

[1] UR3e dataset is obtained in Section III, and KUKA KR200 dataset is available in [41].

includes two forbidden zones: the first being the forbidden zone F, where very low ET cannot be achieved due to limitations in the nominal torque of the actuation system; the second is the forbidden zone S, where very high ET is considered prohibitive since it may have a negative impact on the production rate. In the case of an IR, the EC is calculated using a fourth-degree equation that depends on the task motion time [34]. Tests on IRs demonstrated this tendency in [40], [42]. However, in the case of the cobot UR3e, the relation is linear. The cobot UR3e cannot achieve the non-linear zone of the fourth-degree curve because it moves slower (safety requirements and type of actuators) and is lighter than an IR. Fig. 10 presents the operational graph of both robots.

D. Joint Temperatures

Our observations indicate that the robot consumes slightly less energy when it is warm (see Section III, D - Joint Temperature). Studies on IRs suggest that friction temperature decreases as the oil temperature increases, resulting in a reduction of EC [31]. Similarly, joint temperature affects both types of robots in a similar way.

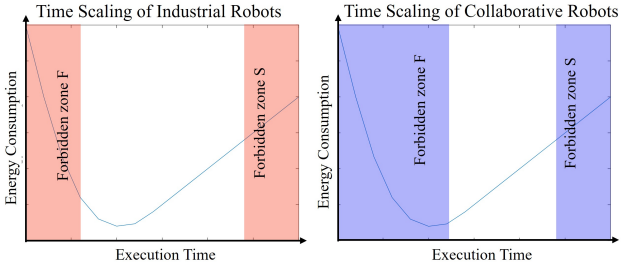

Fig. 10. Time Scaling Zones of IR [40] and cobot UR3e

V. CONCLUSIONS

In this paper, we present a comparative study between industrial robots (IRs) and lightweight robots (LIRs), also known as cobots. First, we review the literature to identify the design differences between these two types of robots. Then, we describe the experimental setups that analyze the energy consumption factors of a cobot, specifically the UR3e. Finally, we compare the energy consumption behavior of the UR3e and IRs from the literature. The results demonstrate that the UR3e and KUKA KR200 exhibit different behaviors in terms of electronics percentage consumption, type of command, and energy signature graph. The UR3e consumes approximately 50% of its energy on electronic components, while the KUKA KR200 consumes only around 6%. Since cobots have lighter structures, mechanical energy consumption is comparable to that of electronic components. In the case of IRs, the energy signature graph (energy consumption vs execution time) is calculated using a fourth-degree equation. However, in the case of the UR3e cobot, the relationship is linear.

The results provide valuable insights into different strategies for optimizing the energy consumption of cobots. For instance, rather than focusing on reducing mechanical energy consumption by path and trajectory planning, efforts should

TABLE IV
COMPARATIVE ANALYSIS TABLE BETWEEN AN IR AND COBOT UR3E

Parameter	Collaborative Robot UR3e	Industrial Robot
Joint Configurations	Using the four positions recommended in [26], UR3e consumes less energy when its links are parallel to the gravity force. UR3e can not release its brakes by command, it has to be activated/deactivated using its teaching pendant.	EC changes according to the robot's position. The IR consumes less energy when its links are parallel to the gravity force [26]. However, for long idle times, IR can use brakes to reduce its EC.
Movement Commands	UR3e using PtP movements consumes less energy than using linear movements.	An IR using PtP movements consumes less energy than using linear movements. [31]
Velocity and Acceleration Limits	UR3e consumes less energy when the velocity and accelerations are the maximum possible value.	In [27], [28] experiments show that the EC changes according to the velocity. Besides, IRs consume more energy when the velocity and accelerations are the maximum possible value [31].
Payload	UR3e consumes more energy when the load increases. A cobot generally has a better ratio of payload to manipulator mass, indicating relatively higher payload capacity.	An IR consumes more energy when the load increases [26], [27], [30], [31], [39]
Electronics Consumption	UR3e consumes around 48 % of its energy on its electronic components.	KUKA KR210 consumes only around 6 % of its energy on the electronic components [31].
Time Scaling	UR3e has a linear relation between EC and task execution time. The cobot only works in the linear zone of the fourth-degree equation. The Forbidden zone F for the UR3e increases due to its safety requirements and actuation system characteristics.	In [34], [40] authors demonstrated a non-linear relationship between EC and task execution time of any manipulator. In [40], authors mentioned two forbidden zones that a manipulator can not achieve due to its limitations.
Joint Temperatures	UR3e EC slightly decreases when the temperature increases.	Experiments in IRs indicate that the EC of the robot decreases when the lubricant temperature increases [26].

be directed toward designing more efficient electronics, such as efficient distribution of computation tasks among the system's assets. The joints of cobots feature microcontrollers and sensors capable of independently controlling each joint motor. Moreover, in certain applications, the computational power of the robot controller is underutilized, and instead, an external computer is responsible for running computationally expensive operations such as machine learning and computer vision.

REFERENCES

[1] ISO 8373:2012 Robots and robotic devices — Vocabulary .

[2] IFR, "World robotics 2022 report," International Federation of Robotics, Tech. Rep., 2022.

[3] B. Singh, N. Sellappan, and P. Kumaradhas, "Evolution of industrial robots and their applications," *International Journal of emerging technology and advanced engineering*, vol. 3, no. 5, pp. 763–768, 2013.

[4] EN ISO 10218-1:2011, Robots and robotic devices — Safety requirements for industrial robots (ISO 10218) .

[5] J. Guiochet, M. Machin, and H. Waeselynck, "Safety-critical advanced robots: A survey," *Robotics and Autonomous Systems*, vol. 94, pp. 43–52, 2017. [Online]. Available: https://www.sciencedirect.com/science/article/pii/S0921889016300768

[6] A. Hentout, M. Aouache, A. Maoudj, and I. Akli, "Human–robot interaction in industrial collaborative robotics: a literature review of the decade 2008–2017," *Advanced Robotics*, vol. 33, no. 15-16, pp. 764–799, 2019.

[7] Kuka, *"Kuka Titan Series Manual"*, 2013. [Online]. Available: https://www.kuka.com/en-de/services//

[8] ABB, *"ABB IRB Series"*, 2021. [Online]. Available: https://new.abb.com/products/robotics/robots/articulated-robots

[9] Kuka, *"Kuka KR 500 Series"*, 2011. [Online]. Available: https://www.kuka.com/en-de/services/

[10] Robotiq, *Collaborative Robots Buyer's Guide*. [Online]. Available: https://blog.robotiq.com/collaborative-robot-ebook

[11] UR, *"Universal Robots e-Series User Manual"*, 2022. [Online]. Available: https://www.universal-robots.com/download

[12] Franka, *"Product Manual Franka Production 3"*, 2022. [Online]. Available: https://www.franka.de/documents/

[13] Kinova, *"User Guide Kinova Gen3 Ultra lightweight robot"*, 2022. [Online]. Available: https://www.kinovarobotics.com/uploads/

[14] F. Sherwani, M. M. Asad, and B. Ibrahim, "Collaborative robots and industrial revolution 4.0 (ir 4.0)," in *2020 International Conference on Emerging Trends in Smart Technologies (ICETST)*, 2020, pp. 1–5.

[15] M. Hägele, K. Nilsson, and J. N. Pires, *Industrial Robotics*. Berlin, Heidelberg: Springer Berlin Heidelberg, 2008.

[16] UR, "Know your machine: Traditional industrial robots vs cobots." [Online]. Available: https://www.universal-robots.com/blog/know-your-machine-traditional-industrial-robots-vs-cobots/

[17] A. Raviola, A. De Martin, R. Guida, G. Jacazio, S. Mauro, and M. Sorli, "Harmonic drive gear failures in industrial robots applications: An overview," in *PHM Society European Conference*, vol. 6, no. 1, 2021, pp. 11–11.

[18] A.-D. Pham and H.-J. Ahn, "High precision reducers for industrial robots driving 4th industrial revolution: state of arts, analysis, design, performance evaluation and perspective," *International journal of precision engineering and manufacturing-green technology*, vol. 5, pp. 519–533, 2018.

[19] G. Hirzinger, A. Albu-Schaffer, M. Hahnle, I. Schaefer, and N. Sporer, "On a new generation of torque controlled light-weight robots," in *Proceedings 2001 ICRA. IEEE International Conference on Robotics and Automation (Cat. No.01CH37164)*, vol. 4, 2001, pp. 3356–3363 vol.4.

[20] A. Angerer, A. Hoffmann, A. Schierl, M. Vistein, and W. Reif, "The robotics api: An object-oriented framework for modeling industrial robotics applications," in *2010 IEEE/RSJ International Conference on Intelligent Robots and Systems*, 2010, pp. 4036–4041.

[21] V. Villani, F. Pini, F. Leali, and C. Secchi, "Survey on human–robot collaboration in industrial settings: Safety, intuitive interfaces and applications," *Mechatronics*, vol. 55, pp. 248–266, 2018. [Online]. Available: https://www.sciencedirect.com/science/article/pii/S0957415818300321

[22] S. El Zaatari, M. Marei, W. Li, and Z. Usman, "Cobot programming for collaborative industrial tasks: An overview," *Robotics and Autonomous Systems*, vol. 116, pp. 162–180, 2019.

[23] J.-F. Lafleche, S. Saunderson, and G. Nejat, "Robot cooperative behavior learning using single-shot learning from demonstration and parallel hidden markov models," *IEEE Robotics and Automation Letters*, vol. 4, no. 2, pp. 193–200, 2019.

[24] K. Fischer, F. Kirstein, L. C. Jensen, N. Krüger, K. Kukliński, M. V. aus der Wieschen, and T. R. Savarimuthu, "A comparison of types of robot control for programming by demonstration," in *2016 11th ACM/IEEE International Conference on Human-Robot Interaction (HRI)*, 2016, pp. 213–220.

[25] Z. Bi, C. Luo, Z. Miao, B. Zhang, W. Zhang, and L. Wang, "Safety assurance mechanisms of collaborative robotic systems in manufacturing," *Robotics and Computer-Integrated Manufacturing*, vol. 67, p. 102022, 2021.

[26] R. R. Garcia, A. C. Bittencourt, and E. Villani, "Relevant factors for the energy consumption of industrial robots," *Journal of the Brazilian Society of Mechanical Sciences and Engineering*, vol. 40, no. 9, pp. 1–15, 2018.

[27] A. Rassõlkin, H. Hõimoja, and R. Teemets, "Energy saving possibilities in the industrial robot IRB 1600 control," *2011 7th International Conference-Workshop Compatibility and Power Electronics, CPE 2011 - Conference Proceedings*, no. 1, pp. 226–229, 2011.

[28] A. Liu, H. Liu, B. Yao, W. Xu, and M. Yang, "Energy consumption modeling of industrial robot based on simulated power data and parameter identification," *Advances in Mechanical Engineering*, vol. 10, no. 5, pp. 1–11, 2018.

[29] M. Brossog, J. Kohl, J. Merhof, S. Spreng, and J. Franke, "Energy consumption and dynamic behavior analysis of a six-axis industrial robot in an assembly system," *Procedia CIRP*, vol. 23, no. C, pp. 131–136, 2014.

[30] M. Gadaleta, M. Pellicciari, and G. Berselli, "Optimization of the energy consumption of industrial robots for automatic code generation," *Robotics and Computer-Integrated Manufacturing*, vol. 57, no. April 2018, pp. 452–464, 2019.

[31] M. Gadaleta, G. Berselli, M. Pellicciari, and F. Grassia, "Extensive experimental investigation for the optimization of the energy consumption of a high payload industrial robot with open research dataset," *Robotics and Computer-Integrated Manufacturing*, vol. 68, no. July 2020, p. 102046, 2021.

[32] M. Pellicciari, A. Avotins, K. Bengtsson, G. Berselli, N. Bey, B. Lennartson, and D. Meike, "AREUS - Innovative hardware and software for sustainable industrial robotics," *IEEE International Conference on Automation Science and Engineering*, vol. 2015-October, pp. 1325–1332, 2015.

[33] S. Riazi, K. Bengtsson, O. Wigström, E. Vidarsson, and B. Lennartson, "Energy optimization of multi-robot systems," *IEEE International Conference on Automation Science and Engineering*, vol. 2015-October, pp. 1345–1350, 2015.

[34] A. Vergnano, C. Thorstensson, B. Lennartson, P. Falkman, M. Pellicciari, C. Yuan, S. Biller, and F. Leali, "Embedding detailed robot energy optimization into high-level scheduling," *2010 IEEE International Conference on Automation Science and Engineering, CASE 2010*, pp. 386–392, 2010.

[35] F. Stuhlenmiller, J. Jungblut, D. Clever, and S. Rinderknecht, "Combined Analysis of Energy Consumption and Expected Service Life of a Robotic System," *2020 6th International Conference on Mechatronics and Robotics Engineering, ICMRE 2020*, pp. 53–57, 2020.

[36] A. Mohammed, B. Schmidt, L. Wang, and L. Gao, "Minimizing energy consumption for robot arm movement," *Procedia CIRP*, vol. 25, no. C, pp. 400–405, 2014.

[37] D. Meike, M. Pellicciari, G. Berselli, A. Vergnano, and L. Ribickis, "Increasing the energy efficiency of multi-robot production lines in the automotive industry," *IEEE International Conference on Automation Science and Engineering*, pp. 700–705, 2012.

[38] EN ISO 9283:1999-05, Manipulating industrial robots - Performance criteria and related test methods (ISO 9283:1998) .

[39] D. Meike and L. Ribickis, "Energy efficient use of robotics in the automobile industry," *IEEE 15th International Conference on Advanced Robotics: New Boundaries for Robotics, ICAR 2011*, pp. 507–511, 2011.

[40] M. Pellicciari, G. Berselli, F. Leali, and A. Vergnano, "A method for reducing the energy consumption of pick-and-place industrial robots," *Mechatronics*, vol. 23, no. 3, pp. 326–334, 2013.

[41] G. Berselli, "Data of the paper: "extensive experimental investigation for the optimization of the energy consumption of a high payload industrial robot with open research dataset"," Aug 2020. [Online]. Available: https://data.mendeley.com/datasets/hdhchngky8/1

[42] D. Meike, M. Pellicciari, and G. Berselli, "Energy efficient use of multirobot production lines in the automotive industry: Detailed system modeling and optimization," *IEEE Transactions on Automation Science and Engineering*, vol. 11, no. 3, pp. 798–809, 2014.